Conf-930956--2

Microanalysis of an oxidized cobalt oxide - zirconia eutectic

J. Bentley, S. McKernan*, C. B. Carter* and A. Revcolevschi†

Metals and Ceramics Division, Oak Ridge National Laboratory, P.O.Box 2008, Oak Ridge, TN 37831-6376
*Department of Chemical Engineering and Materials Science, University of Minnesota, 421 Washington Avenue SE, Minneapolis, MN 55455-0132
†Laboratoire de Chimie des Solides, Université de Paris-Sud,Bâtiment 414, F-91405 Orsay Cedex, France.

ABSTRACT: The compositions of CoO, Co_3O_4, and Ca-stabilized cubic ZrO_2 in an oxidized directionally solidified CoO-ZrO_2 eutectic were determined by PEELS and EDS. An oxygen gradient exists across the Co_3O_4 with highest levels near the ZrO_2 interface. Oxygen ELNES for CoO and Co_3O_4 are quite different; published oxygen ELNES have been incorrectly attributed to CoO. Normalized Co-L_{23} white line intensity (WLI) ratios for CoO and Co_3O_4 are similar (0.53 ± 0.02) but L_3/L_2 WLI ratios are 3.88 and 2.58, respectively. ELCE data suggest Co_3O_4 has the inverse spinel structure.

1. INTRODUCTION

The morphology of directionally solidified eutectics (DSE) provides an excellent geometry for studying interfaces in materials. Dravid et al. (1989) have studied interface structures in a NiO-ZrO_2(CaO) DSE with high-resolution transmission electron microscopy (TEM). The thin, parallel plates which are formed in the ZrO_2/CoO system also produce flat interfaces on the microscopic scale. However, heat treatment of the eutectic in a high oxygen partial pressure results in a trilayer structure as the CoO transforms to Co_3O_4. The microstructure, illustrated in Fig. 1, consists of alternating lamellae of CoO and calcium-stabilized cubic-ZrO_2, each with widths of up to 1 μm, and a thin (100 to 200 nm), irregular layer of Co_3O_4 spinel extending into the CoO from the flat ZrO_2 interface. The growth direction of the DSE is $[001]_{ZrO2}$ // $[1\bar{1}0]_{CoO}$ and the broad interface is $(100)_{ZrO2}$ // $(111)_{CoO}$. The Co_3O_4 is oriented cube-on-cube with the CoO.

2. EXPERIMENTAL

Analytical electron microscopy (AEM) was performed at ORNL with a Philips EM400T AEM equipped with a field emission gun (FEG), a Gatan 666 parallel-detection electron energy-loss spectrometer (PEELS) system, and an EDAX 9100 energy dispersive X-ray spectrometer (EDS). Philips CM12/STEM (equipped with an EDAX light element (SUTW) EDS detector and 9900 analyzer) and CM30/STEM AEMs were also used. For microanalysis, Gatan double-tilt cooling holders were used at -130°C.

3. COMPOSITION DETERMINATION

Typical results of the microanalysis of the stabilized cubic zirconia phase by PEELS and EDS are

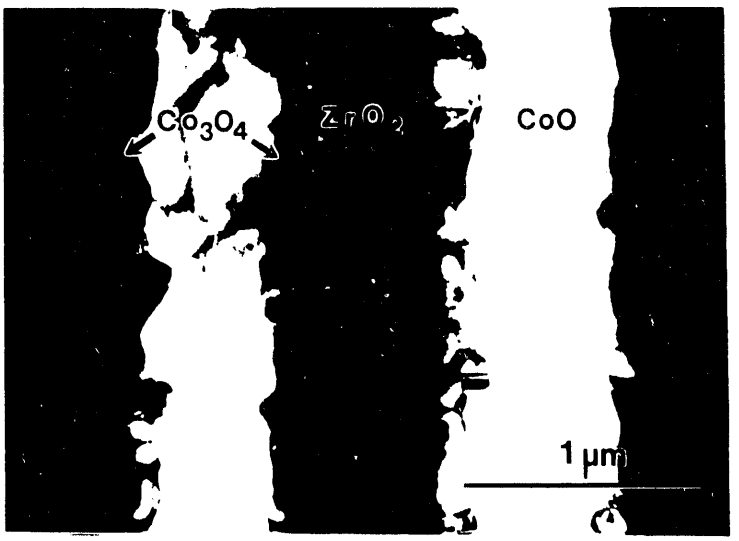

Fig. 1. Oxidized CoO-ZrO_2 directionally solidified eutectic showing lamellae of CoO and ZrO_2 with irregular interface layer of Co_3O_4.

shown in Fig. 2. For PEELS, the proximity of the Zr M_3 and overlap with the Zr M_2 preclude accurate use of the Ca L_{23} edge for composition determination (see Fig. 2a), but fortunately Ca/Zr ratios are easily obtained by EDS (Fig. 2b). Such measurements indicate that the Ca/Zr atomic ratio is 0.18. However, for other aspects of composition determination, secondary excitation in EDS gives misleading results, such as the apparent presence of zirconium in the cobalt oxides and higher than actual levels of cobalt in the zirconia (Fig. 3). Accurate quantification of oxygen contents from the EDS data was limited by the large absorption corrections that are necessary. Thus, as is common, a combination of AEM techniques works best.

Typical PEELS data for the cobalt oxide phases are shown in Fig. 4. To accurately determine compositions (Egerton 1986), care has to be taken in the treatment of the energy-loss near-edge structure (ELNES), e.g., the Co L_{23} "white lines." A simple approach, that of beginning the integration window just beyond the most pronounced ELNES was used. The measured values of composition depend upon the position of the integration window and the use of the white line correction in the Gatan EL/P (version 2.1) software. A 100 eV integration window offset from the edge threshold by 25 eV gave the most reliable results. Further work, at higher spatial resolution, indicated a reproducible ~2% gradient in the Co:O ratio across the Co_3O_4 phase with the lowest values (highest oxygen content) near the ZrO_2 interface. This is consistent with the proposed mechanism of phase formation that is based on rapid diffusion of oxygen in the ZrO_2 lamellae and slower lateral diffusion into the cobalt oxide. The measurement of such composition gradients is possible because the precision is much better than the absolute accuracy of the data.

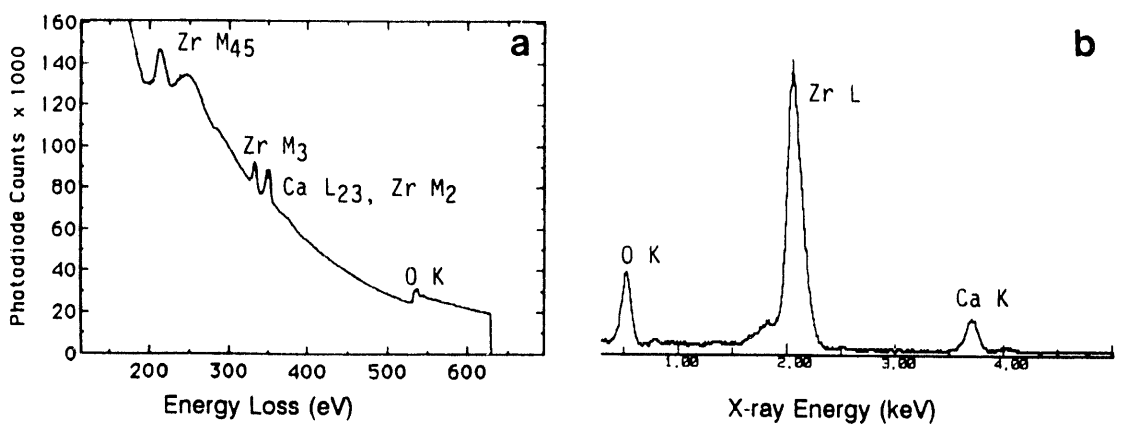

Fig.2. Microanalysis of the zirconia phase by (a) PEELS and (b) EDS.

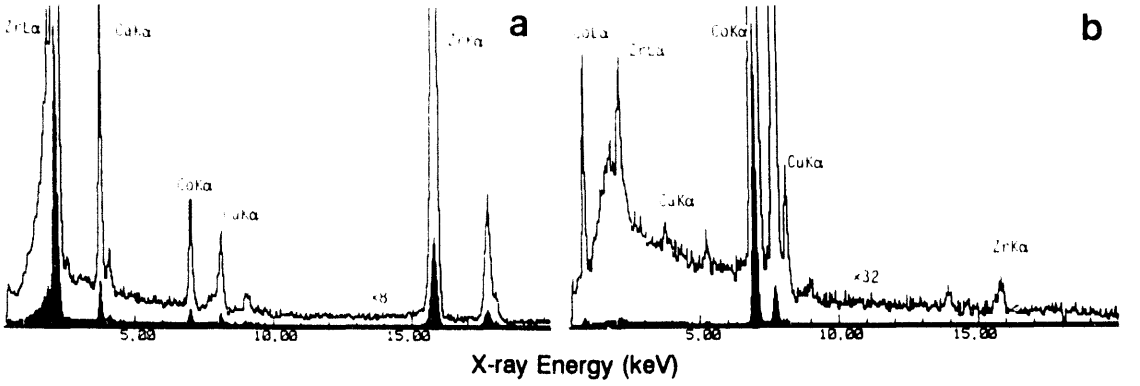

Fig.3. X-ray microanalysis showing effects of secondary excitation. (a) higher than expected levels of Co in zirconia and (b) apparent presence of Zr in CoO.

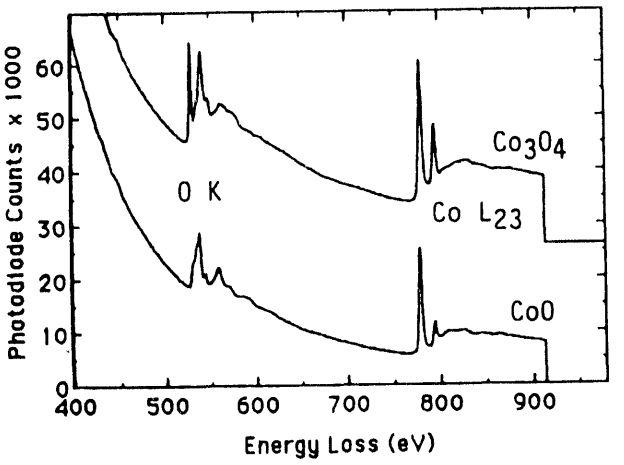

Fig.4. PEELS data from CoO and Co_3O_4.

4. NEAR EDGE STRUCTURES

Inspection of the oxygen energy-loss near-edge structure (ELNES) reveals dramatic differences between the CoO and Co_3O_4 (Fig. 5a). Interpretation of such oxygen ELNES is complex and involves consideration of site symmetry and states arising from hybridization of oxygen 2p levels with metal 3d and 4s or 4p levels (de Groot et al. 1989). Nevertheless, the differences in oxygen ELNES provide easily identifiable signatures for the two cobalt oxides. The cobalt $L_{2,3}$ ELNES (Fig. 5b) is superficially similar for the two phases, but there is a small shift to higher energies for the Co_3O_4 (~1.5 eV for the L_3, ~0.6 eV for the L_2). The normalized white line intensity (WLI) ratio, relative to the continuum states in a 50 eV window, 50 eV above the L_3 edge (Pearson et al. 1988), is 0.53 ± 0.02 for the two cobalt oxides, implying similar 3d occupancies. The L_3/L_2 WLI ratios are 3.88 and 2.58 for the CoO and Co_3O_4, respectively. From the type of analysis employed by Morrison et al. (1985), the ratios of 5/2 to 3/2 state holes are 1.42 and 0.89 for CoO and Co_3O_4, respectively, and the ratio of the total number of 3d holes in CoO to those in Co_3O_4 is 0.98, in agreement with the normalized WLI ratio analysis. Quantitative measurements were made on single scattering profiles, but difficulty was experienced in implementing even the simple geometric approach used by Pearson et al. (1988) because of the edge shape just beyond the white lines.

Oxygen and cobalt ELNES (at a higher energy resolution than our present results) for cobalt oxide have recently been published (Krivanek and Paterson 1990). The results were stated as being for CoO (made by oxidizing thin evaporated metal films in air at 400°C). However, the

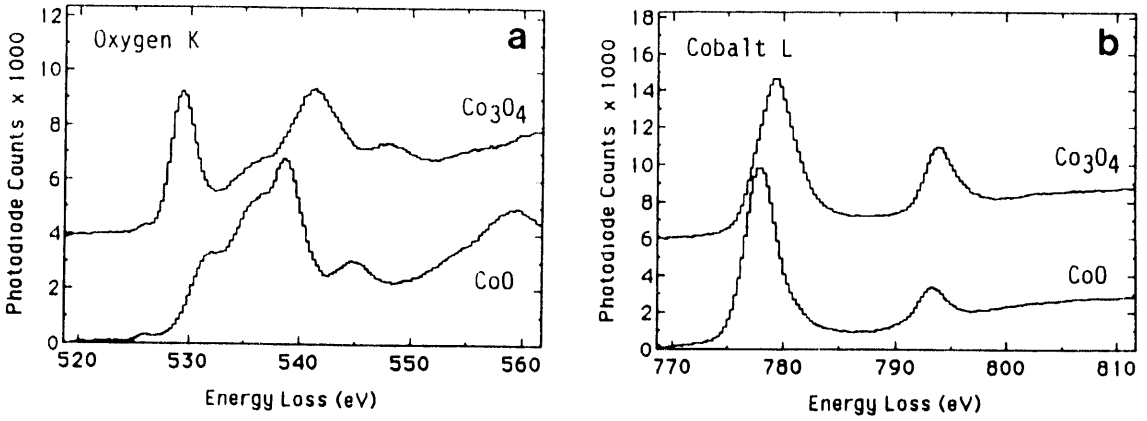

Fig.5. (a) Oxygen and (b) cobalt-L near-edge fine structures for CoO and Co_3O_4.

published oxygen ELNES is not at all like our results for CoO; rather, there is excellent agreement with our results for Co_3O_4. Similarly, the positions of the published Co L white lines are more consistent with our data for Co_3O_4 than CoO. Phase diagram data indicate that Co_3O_4 is the stable oxide below ~900°C for oxygen partial pressures of >0.1 atm.

Krivanek et al (1982) extended the EDS-based ALCHEMI (atom location by channeling-enhanced microanalysis) method to demonstrate energy-loss with channeled electrons (ELCE) for $MgAl_2O_4$ spinel. Tafto and Krivanek (1982) further extended the method to demonstrate site-specific valence determination of Fe in a chromite spinel. Similar experiments were performed in an attempt to discriminate the signature of the di- and tri-valent cobalt ions in Co_3O_4. Although Co:O intensity ratios varied in the expected manner, no difference in the Co ELNES was detected. The most likely explanation for this behavior is that Co_3O_4 has the inverse spinel structure. There is some supporting evidence from X-ray diffraction data on bond lengths; in addition, Fe_3O_4 has the inverse spinel structure. Further experiments are planned.

ACKNOWLEDGEMENTS

This research was supported by the Division of Materials Sciences, U.S. Department of Energy under contract DE-AC05-84OR21400 with Martin Marietta Energy Systems, Inc. and through the SHaRE program under contract DE-AC05-76OR00033 with Oak Ridge Associated Universities, and by NSF under grant #DMR-8901218.

REFERENCES

Dravid V P, Lyman C E, Notis M R and Revcolevschi A 1989 Ultramicroscopy **29** 60-70
Egerton R F 1986 EELS in the Electron Microscope (New York: Plenum)
de Groot F M F, Grioni M, Fuggle J C, Ghijsen J, Sawatzky G A and Petersen H 1989 Phys. Rev. B **40** 5715-23
Krivanek O L, Disko M M, Tafto J and Spence J C H 1982 Ultramicroscopy **9** 249-254
Krivanek O L and Paterson J H 1990 Ultramicroscopy **32** 313-8
Morrison T I, Brodsky M N, Zaluzec N J and Sill L R 1985 Pys. Rev. B **32** 3107
Pearson D H, Fultz B and Ahn C C 1988 Appl. Phys. Lett. **53** 1405
Tafto J and Krivanek O L 1982 Phys. Rev. Lett. **48** 560

DISCLAIMER

END

DATE FILMED

4/5/94